文章编号:1006-9941(2022)05-0491-11

Combined ARC-MS Study and ReaxFF Molecular Dynamics Simulations on Thermal Decomposition Mechanisms of DNP

LAN Guan-chao[1,2], ZHANG Lin-sheng[1], LIU Xue-ying[2], CHAO Hui[2], LI Zhi-hua[2], CAO Duan-lin[1], WANG Jian-long[1]

(1. *School of Chemical Engineering and Technology, North University of China, Taiyuan* 030051, *China*; 2. *Gansu Yin Guang Chemical Industry Group Co. Ltd, Baiyin* 730900, *China*)

Abstract: ReaxFF molecular dynamics (ReaxFF MD) simulations were adopted to identify the main intermediate products, final products and chemical reactions during 3,4-dinitro-1*H*-pyrazole (DNP) thermal decomposition. Accelerating rate calorimeter (ARC)-mass spectrometer (MS) technique was adopted to study DNP thermal decomposition properties and identify the gaseous products. The simulated results illustrate that $C_3HO_4N_4$, $C_3HO_3N_4$, $C_3HO_2N_3$, C_3HNO_2, NO_2 are the main intermediate products, and H_2O, CO_2, N_2 are the main final products. MS detected main gaseous products are H_2O, CO_2, N_2 as well. According to the simulation results, the produced time and abundance of the products are obtained as well. Among which $C_3HO_3N_4$ is the first generated intermediate product, and H_2O is the first generated final product. $C_3HO_3N_4$ and N_2 are the intermediate and final products with the largest amount, respectively. Additionally, the main chemical reactions in DNP thermal decomposition process are also acquired by molecular dynamics simulations. According to the generation time and abundance of products, the decomposition path of DNP was obtained.

Key words: 3,4-dinitro-1*H*-pyrazole (DNP); ReaxFF MD simulations; ARC-MS technique; thermal decomposition mechanism

CLC number: TJ55 **Document code**: A **DOI**: 10.11943/CJEM2021190

1 Introduction

Melt cast explosives, the most widely used explosives in both the military and the civilian area, can be used to fill mortars, grenades, artillery shells, warheads and antipersonnel mines[1]. With the development of weapon systems, modern melt cast explosives have to meet different requirements depending on their applications such as high energetic performance, high density, low sensitivity toward external stimuli and low thermal hazards[2]. The carriers with high density can enhance the detonation performances of melt cast explosives, and the carriers with low sensitivity can improve the safety of melt cast explosives. Therefore, it's necessary to obtain a candidate carrier to meet the requirements of modern munition on energy and safety.

3,4-Dinitro-1*H*-pyrazole(DNP) is a good candidate of melt cast explosives carrier, whose melting point, friction sensitivity, density and detonation velocity are 87 ℃[1], 360 N[2], 1.81 g·cm^{-3}[1] and 8.24 km·s^{-1}[1], respectively. The detonation velocity of DNP is higher than that of TNT (6.94 km·s^{-1}) and the mechanical sensitivity of DNP is lower than that of DNAN, indicating that DNP could be a potential energetic material as melt cast explosive carrier to replace TNT and DNAN. It has been proved that DNP could already replace TNT as melt cast explosives in compositions such as Composition B (RDX/TNT)[3]. Therefore, DNP has broad application prospects as melt cast explosive carrier. Many researches have reported the synthesis, recrystallization, physicochemical properties and application of DNP[2-6]. However, no researches report the thermal decomposition

Received Date: 2021-07-17; **Revised Date**: 2021-10-16

Published Online: 2022-03-31

Bipgraphy: LAN Guan-chao (1989-), male, doctor, majoring in the crystallization of energetic materials。e-mail:gclan@nuc.edu.cn

引用本文:兰贯超,张琳升,刘学英,等. DNP热分解机理的ReaxFF模拟[J]. 含能材料,2022,30(5):491-501.

LAN Guan-chao, ZHANG Lin-sheng, LIU Xue-ying, et al. Combined ARC-MS Study and ReaxFF Molecular Dynamics Simulations on Thermal Decomposition Mechanisms of DNP[J]. *Chinese Journal of Energetic Materials (Hanneng Cailiao)*, 2022, 30(5):491-501.

path and decomposition products of DNP by experiments or simulations. Thermal decomposition mechanisms play important role in studying thermal safety of energetic materials. According to the decomposition path and products, some effective methods can be acquired to prevent the decomposition of energetic materials. It's difficult to obtain a detailed understanding of energetic materials decomposition process by experiments or simulations, in that the thermal decomposition is complex. Experiments can examine the accuracy of simulations, and simulations can provide some information that can't be measured by experiments. Combined experiments and simulations, intermediate products, final products and chemical reactions of DNP thermal decomposition can be obtained to analyze the decomposition mechanism.

ReaxFF molecular dynamics (ReaxFF MD) simulations is a good method to study the pyrolysis characteristic of materials[7-11]. ReaxFF MD simulations have developed to one of the main techniques for exploring the reaction of condensed phase using reactive force fields[12-13]. ReaxFF MD simulations have been successfully applied to study the thermal decomposition of many energetic materials, such as TATB(1,3,5-triamino-2,4,6-trinitrobenzene), RDX (trinitro-1, 3, 5-triazacyclohexane), TKX-50 (dihydroxylammonium 5, 5′-bistetrazole-1, 1′-diolate), HMX(1,3,5,7-tetranitro-1,3,5,7-azacyclo-octane), CL-20 (1, 3, 5-hexanitrohexaazaisowurtzitane) and PETN (pentaerythritol tetranitrate) and so on[12-18].

TG-MS (thermogravimetric-mass spectrometer) is a commonly used method to confirm the gaseous products produced by materials pyrolysis. However, this method is not suitable for studying DNP, in that DNP is evaporated before it decomposed at 100 kPa as the low melting point of DNP. Therefore, in this study, accelerating rate calorimeter (ARC) was used to investigate the decomposition of DNP in the closed system, and the gaseous products were gathered after the decomposition of DNP. MS technique was used to identify the gathered gaseous products. Then, the main intermediate products, main final products and main chemical reactions were analyzed by ReaxFF MD simulations at 2000, 2500 K and 3000 K, respectively. Based on the evolution of products and reactions, thermal decomposition mechanisms of DNP are obtained.

2 Experiments and simulations

2.1 Chemical materials and instruments

DNP sample was synthesized in the laboratory. It was purified by recrystallization and measured by High Performance Liquid Chromatography. The purity was greater than 0.995. ARC from NETZSCH Co., Ltd using a 1/4-inch hastelloy C vessel with a thermocouple clip located on the bottom of the vessel was used. MS spectra (NETZSCH QMS 403D Germany) worked in two scanning functions, including full scanning mode and selected ion recording (MID) mode. The MS signals of all the fragment ions were detected by the former mode and the MID mode tracked MS signals of some specific ions marked accurately like m/z 18 and 28.

2.2 ARC-MS measurements

ARC was adopted to investigate DNP thermal decomposition in the closed system. 194.4 mg DNP samples were placed in a spherical hastelloy C vessel with a volume of 10 mL and a mass of 21.5 g, and the standard 'heat-wait-search' procedure was used for the measurement with temperature increments of 5 ℃. At each step, the system was kept adiabatic for a 'wait' period until thermal transients disappeared and then placed in 'search' mode, looking for an exotherm. ARC experiments were started at 50 ℃ and the apparatus would repeat the heat-wait-seek model until the temperature reached 350 ℃.

The gaseous products produced by DNP were gathered when the temperature of spherical hastelloy C vessel of ARC decreased to 100 kPa. Then, the m/z of the gathered gaseous products were analyzed by MS technique. Full scanning mode of MS technique with m/z between 1 and 400 was adopted to detect MS signals of all fragment ions. Based on the experimental results, final gaseous products

were identified. Before scanning, pure argon was pumped to MS apparatus for 1 h to remove the air and create an inert atmosphere.

2.3 ReaxFF MD simulations

2.3.1 Simulations details

In this study, the isothermal decompositions of DNP were studied by large-scale atomic/molecular massively parallel simulator (LAMMPS)[19] using ReaxFF-lg reactive force field[12-13] at different temperature. The crystal structure of DNP belongs to monoclinic system with the lattice parameters of a=9.70 Å, b=12.08 Å, c=9.76 Å, and β=93.96°[20]. A 3×3×3 DNP supercell (Fig. 1, 216 molecules, 2808 atoms) was used to study the thermal decompositions process of DNP at different temperature. In order to relax the internal stress of DNP, 10 ps molecular dynamic simulations were first performed with NVT ensemble at 298 K using ReaxFF-lg force field, and then another 10 ps molecular dynamic simulations were performed with NPT ensemble at 298 K and 100 MPa using ReaxFF-lg force field[12]. Then, 400 ps, 200 ps and 100 ps MD simulations were performed at 2000, 2500 K and 3000 K, respectively, with NVT ensemble using ReaxFF-lg force field to study the decomposition properties of DNP. The temperature and pressure were controlled by using the Nosé-Hoover thermostat and barostat, respectively. As the bond orders and charge will be calculated after each reactive molecular dynamic simulation step, small integration time step should be adopted for efficient coverage of the phase space allowing collisions and reaction to occur smoothly[12, 21]. In this study, the time step was set to 0.1 fs, and the dynamic trajectory was recorded every 200 fs. These collected simulation values were used to identify the species produced by DNP to provide information for analysis chemical reactions[22].

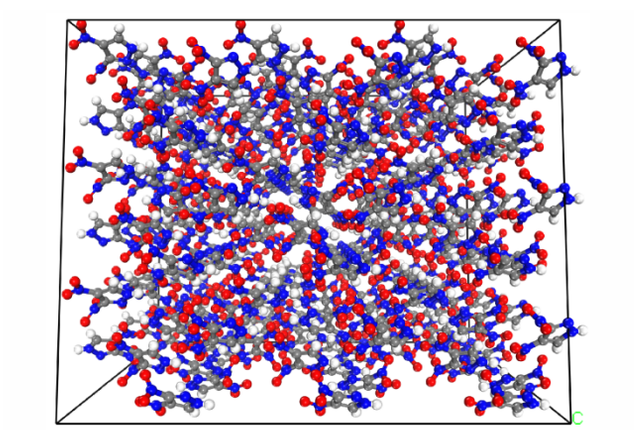

Fig.1 Crystal structure of DNP

2.3.2 Reaction kinetic parameter analysis

DNP thermal decomposition process includes three reaction steps: initial pyrolysis stage, intermediate pyrolysis stage, and final product evolution stage[23-24]. The initial pyrolysis stage and pyrolysis stage are divided at the time when potential energy (E_p) of DNP reaches the highest (t_{max}). The relationship between DNP thermal decomposition reaction rate constant and temperature can be described by linear Arrhenius function (Eq.1)[25].

$$\ln(k) = \ln(A) - \frac{E_a}{RT} \tag{1}$$

where k, A, E_a, R and T represent rate constant, pre-exponential factor(s^{-1}), activation energy(kJ·mol^{-1}), universal gas constant(8.314 J·mol^{-1}·K^{-1}) and temperature (K), respectively.

The rate constant of DNP initial decomposition stage (k_1) can be calculated by Eq. 2 from the beginning of DNP decomposition t_0 to t_{max}.

$$N_t = N_0 \exp\left[-k_1\left(t - t_0\right)\right] \tag{2}$$

where N_t is DNP molecules number, N_0 is DNP molecules initial number, and t_0 is the time when DNP begins to decompose(ps). Then, E_a and A of DNP initial decomposition stage can be calculated by Eq.1.

The rate constant of DNP intermediate decomposition stage (k_2) can be calculated by Eq. 3 from t_{max}.

$$U_t = U_\infty + (U_{t_{max}} - U_\infty)\exp\left[-k_2\left(t - t_{max}\right)\right] \tag{3}$$

where U_t is E_p value ,kcal·mol^{-1}, U_∞ is Ep asymptotic value, kcal·mol^{-1}, $U_{t_{max}}$ is E_p maximum value, kcal·mol^{-1}. Then, E_a and A of DNP intermediate decomposition stage can be obtained by Eq. 1.

The rate constant of final product evolution stage (k_3) can be calculated by Eq. 4 from the formation time of the product.

$$C_t = C_\infty\left\{1 - \exp\left[- k_3\left(t - t_i\right)\right]\right\} \quad (4)$$

where C_∞ is final product molecules asymptotic amount, t_i is the formation time of the product (ps). Then, E_a and A of final products can be obtained by Eq. 1.

3 Results and discussion

3.1 ARC-MS analysis

3.1.1 ARC analysis

In this study, ARC is used to study the decomposition properties of DNP in the closed system, and the gaseous products are gathered after the decomposition at room temperature. The variation of temperature (T) and pressure (p) with time (t) during the whole measurements are displayed in Fig.2, and the temperature change rate (dT/dt) and pressure change rate (dp/dt) with time (t) during DNP decomposition process are depicted in Fig. 3. The measured T_0 (initial decomposition temperature), T_f (final decomposition temperature), ΔT_{ad} (adiabatic temperature rise), β_0 (initial temperature rise rate), β_m (maximum temperature rise rate), t_m (time to maximum temperature rise rate), T_m (temperature of maximum temperature rise rate), p_0 (initial decomposition pressure), p_f (final decomposition pressure) and p_m (maximum pressure rise rate) are summarized in Table 1.

It can be concluded from Fig. 2 that when the temperature is below T_0 the pressure increases slowly. When DNP start to decompose, the temperature and pressure rise rate are gradually increased. Fig. 3 shows that two peaks exist on the dT/dt and dP/dt curves, illustrating that the decomposition of DNP can be divided into two steps. The first step is the decomposition of DNP to produce intermedia products, and the second step is the reaction between the interaction products. Table 1 illustrates that the T_0 of DNP is higher than that of TNT (2, 4, 6-trinitrotoluene, 200.9 ℃) but lower than that of DNAN (1-methoxy-2, 4-dinitro-benzene, 232.0 ℃)[26], indicating that the thermal stability of DNP is higher than that of TNT and lower than that of DNAN. ΔT_{ad} and β_m of DNP are lower than TNT (135.4 ℃, 811.9 ℃·min^{-1}) and DNAN (125.9 ℃, 14.9 ℃·min^{-1}), and t_m of DNP is higher than TNT (883.1 min) and DNAN (898.7 min), illustrating that the thermal hazardous of DNP is lower than TNT and DNAN. In addition, the P_m of DNP is lower than TNT (9.74 MPa·min^{-1}) and DNAN (1.14 MPa·min^{-1}), illustrating that the thermal safety of DNP is higher than those of TNT and DNAN. The time to maximum temperature rise rate (t_m) of DNP is long, demonstrating that the decomposition rate of DNP is low. Moreover, the initial decomposition pressure (P_0) of DNP is 0.302 MPa that is higher than 0.165 MPa (the pressure of air heated to T_0), illustrating that some DNP are evaporated before thermal decomposition. In Fig.2, when temperature is below the melting point of DNP (T_m, 87 ℃),

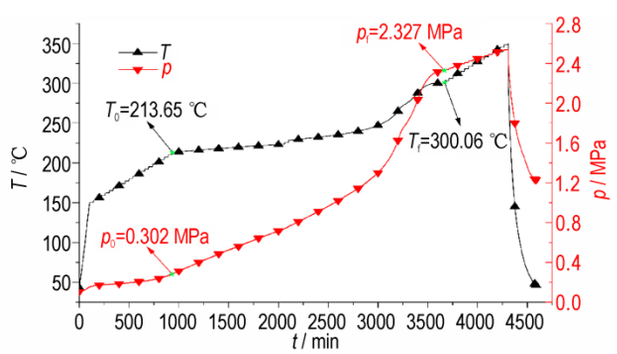

Fig.2 Curves of p-t and T-t during the whole measurements

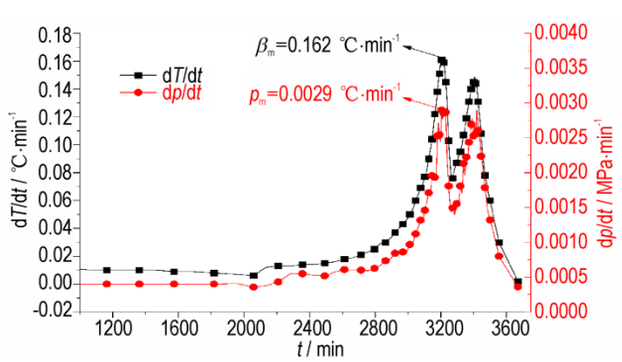

Fig.3 Curves of dT/dt-t and dp/dt-t during the decomposition process of DNP

Table 1 ARC measured thermal decomposition parameters of DNP

Parameters	T_0/℃	ΔT_{ad}/℃	β_m/℃·min^{-1}	T_m/℃	P_f/MPa	T_f/℃	β_0/℃·min^{-1}	t_m/min	P_0/MPa	P_m/MPa·min^{-1}
Value	213.65	86.41	0.162	266.73	2.327	300.06	0.01	2241.44	0.302	0.0029

the pressure rise of the system is contributed by the temperature rise. When the temperature is between T_m and T_0, the evaporation of DNP will contribute to the pressure rise of the system. Therefore, if thermal decomposition properties of DNP are studied in an open system, most of DNP are evaporated and thermal decomposition products can't be obtained.

3.1.2 MS analysis

MS technique is used to analyze the gathered gaseous products produced by DNP decomposition in ARC. Full scanning mode of MS technique with *m*/*z* from 1 to 400 is performed to analyze the *m*/*z* of the gathered gaseous products generated by DNP pyrolysis. The obtained MS spectrum of DNP thermal decomposition products is shown in Fig. 4. As no products with *m*/*z* greater than 60 are detected, Fig.4 displays the products with *m*/*z* from 1 to 60.

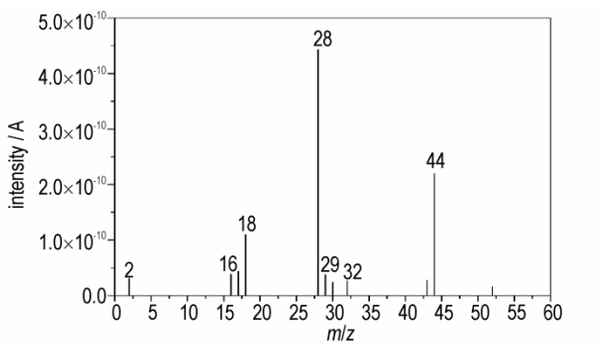

Fig.4 MS spectrum of DNP thermal decomposition products

It can be concluded from Fig. 4 that the main MS peaks are *m*/*z*=18, 28 and 44. The gaseous products are gathered at ambient temperature resulting in that some H_2O (*m*/*z*=18) are condensed to liquid state and the content of H in DNP molecule is low, which results in the low intensity of H_2O. Since DNP only contains C, H, O and N four kinds of atoms, the species with *m*/*z* of 28 can be assigned N_2 or CO or the composite of N_2 and CO, and the species with *m*/*z* of 44 can be assigned to CO_2. In addition, some other gaseous products with low concentration are also detected such as *m*/*z*=2, 16, 17, 29, 30, 32 and 43. Among which, *m*/*z*=32 can be assigned to O_2 (originating from air) that may be introduced to the gas cartridge when we gather the gaseous products. The species with *m*/*z* of 2 can be assigned to H_2, because there are no other species with *m*/*z* of 2. The species with *m*/*z* of 16 and 17 can be assigned to CH_4 and NH_3, respectively. Typical fragments corresponding to the possible species are list in Table 2. As the gaseous products were gathered and analyzed at room temperature rather than their generation time, resulting in that some gaseous products condensed to condensed state such as H_2O and some unstable ionic products react with each other to form condensed or other products such as NO_2. In addition, some products may have the same *m*/*z* such as N_2 and CO. These phenomena will result in MS experimentally measured gaseous products are less than the real situations. In order to study the real time products, ReaxFF MD simulations are adopted in this study.

Table 2 Typical fragments corresponding to the possible species

m/*z*	Assignments	*m*/*z*	Assignments
2	H_2^+	30	CH_2O^+, $C_2H_6^+$, CH_4N^+
16	CH_4^+	32	O_2^+
17	NH_3^+	43	$C_3H_7^+$,$C_2H_5N^+$,$C_2H_3O^+$,$CHON^+$
18	H_2O^+	44	CO_2^+
28	N_2^+,CO^+,$C_2H_4^+$,CH_2N^+	52	$C_2N_2^+$
29	CHO^+, $C_2H_5^+$, CH_3N^+		

3.2 ReaxFF MD simulations

3.2.1 Validation of the accuracy of ReaxFF

ReaxFF simulated density and cell parameters of DNP are compared with X-ray single-crystal diffraction experimental results to examine the accuracy of ReaxFF in describing DNP. The simulated density and cell parameters of DNP together with experimental data are shown in Table 3. ReaxFF simulated density and cell parameters of DNP show great agreement with the XRD results, demonstrating that ReaxFF simulation is reliable.

Table 3 Lattice parameters and density of DNP.

Parameters	ReaxFF	exp	deviation%
a/Å	9.822	9.701	1.247
b/Å	12.230	12.080	1.242
c/Å	9.880	9.759	1.240
β/(°)	93.962	93.962	0.000
ρ/g·cm^{-3}	1.773	1.841	−3.694

3.2.2 Evolution of potential energy and total number of DNP

The evolution of E_p of DNP can be used to determine whether a chemical reaction reaches equilibrium, in that E_p is related to the molecular interactions and relative position[18]. Total number of DNP molecules can be used to evaluate the degree of the thermal decomposition. In this study, within 400 ps, 200 ps and 100 ps simulations, the E_p of DNP reach equilibrium at 2000 K, 2500 K and 3000 K, respectively. The evolutions of E_p and total number of DNP molecules with time at different temperatures are shown in Fig.5.

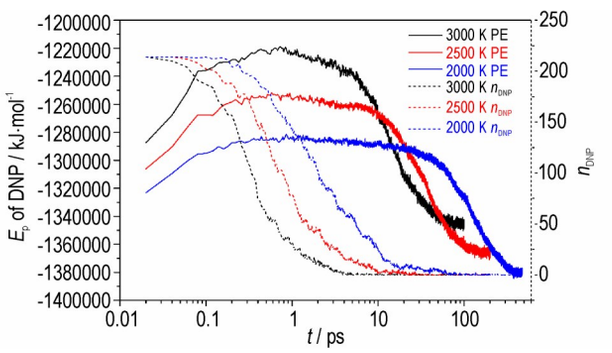

Fig.5 Evolutions of E_p (solid lines) and total number of DNP molecules (dash lines) with time at different temperatures

The simulated E_p curves illustrate that the E_p of DNP at each temperature reaches a maximum value within a short time indicating that DNP will absorb energy before the decomposition. Then, E_p gradually decreases, which means that the exothermic decomposition of DNP is in progress. Finally, the E_p tends to constant demonstrating that all DNP molecules have decomposed and chemical reactions between intermediate products reach equilibrium. It can be concluded from the simulated E_p curves that at high temperature DNP molecules absorb energy to reach its thermal decomposition activation energy initially, and then DNP molecules start to decompose and release energy until the reaction reaches equilibrium. Moreover, at higher temperature, the maximum E_p values, the E_p decrease rates and the stable E_p values are higher, and the time of the chemical reaction reaching equilibrium is shorter, illustrating that high temperature is conducive to DNP decomposition. The curves of total number of DNP molecule show that higher temperature cause faster decrease of DNP molecule indicating a higher decomposition rate. Generally, the decomposition process of an explosive can be divided into two steps: the first step is the decomposition of explosive molecules to generate intermediate products, and the second step is the reaction between intermediate products to form final products[27]. It can be concluded from Fig.5 that the E_p of DNP decrease rapidly when the total number of DNP tend to zero demonstrating that the second step releases more energy than the first step during the DNP decomposition, and the released energy of DNP decomposition is mainly originating from the reaction between intermediate products.

3.2.3 Evolution of intermediate and final products

The simulation results show that a large number of intermediate and final products are produced during the thermal decomposition of DNP. Final simulated configuration of the decomposition products of DNP after 400 ps at 2000 K are displayed in Fig.6.

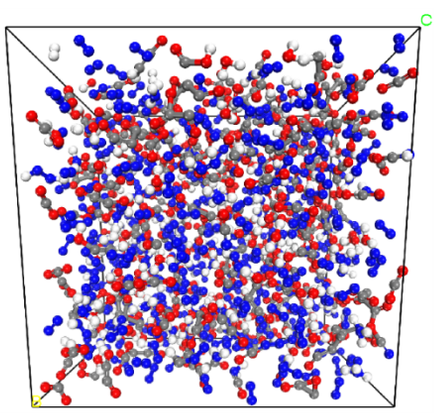

Fig.6 Final products of DNP decomposition

Fig. 6 illustrates that there are no DNP molecules existence after 400 ps ReaxFF MD simulation at 2000 K, and the main intermediate products ($C_3HO_4N_4$, $C_3HO_3N_4$ and NO_2 etc.) produced by DNP react with each other formed stable final products after 400 ps simulation at 2000 K. The final products produced by DNP are small molecular products such as N_2, H_2O, CO_2, H_2, NH_3, C_2O_2 etc. Among which 52.2 percentages (mass fraction) are N_2, H_2O, CO_2 illustrating that the main products

are N_2, H_2O, CO_2 during the decomposition of DNP, which is similar with the experimental results. The decomposition mechanism of DNP can be deduced by the abundance and generation time of intermediate and final products. Fig.7 shows the simulated generation time of main unstable intermediate and stable final products during DNP decomposition at 2000 K. Fig.8 shows the abundance evolution of main unstable intermediate products ($C_3HO_4N_4$, $C_3HO_3N_4$, $C_3HO_2N_3$, C_3HNO_2, NO_2) and final stable products (N_2, H_2O, CO_2) generated by DNP during thermal decomposition at 2000 K.

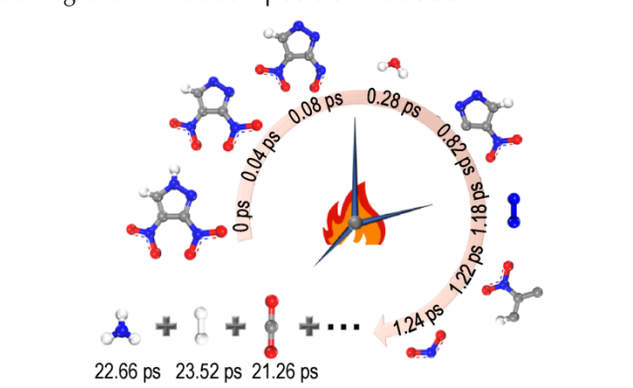

Fig.7 Main intermediates and final products generated by DNP decomposition at 2000 K

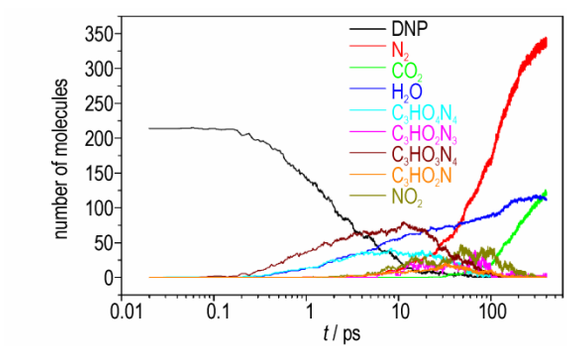

Fig.8 The evolutions of the amounts of the main intermediates and final products generated by DNP decomposition at 2000 K

Fig.7 illustrates that the chronological orders of the appearance of intermediate and final products are $C_3HO_4N_4$, $C_3HO_3N_4$, $C_3HO_2N_3$, C_3HO_2N, NO_2 and H_2O, N_2, CO_2, NH_3, H_2, respectively. The simulated chronological orders can provide important guidance for studying the decomposition path of DNP, which is difficult to obtain by experiment. Fig. 8 illustrates that with the reactions going on the abundance of the intermediate products $C_3HO_4N_4$, $C_3HO_3N_4$, $C_3HO_2N_3$, C_3HO_2N and NO_2 molecules first increase and then gradually decrease to zero, because these intermediate products react with each other or react with DNP to form stable products. In the initial decomposition stage of DNP, the main intermediate products are $C_3HO_4N_4$, which are produced by the decomposition of DNP. With the decomposition going on, the main intermediate products change to $C_3HO_2N_3$, C_3HN_2 and NO_2, that are generated by the reactions between intermediate products. After 300 ps simulations, intermediate products decrease to zero, illustrating that intermediate decomposition stage of DNP has completed. H_2O molecules are generated at 0.28 ps which is earlier than the appearance of $C_3HO_2N_3$, C_3HN_2 and NO_2, indicating the generation of H_2O molecules is undergoing during the whole decomposition process. After 280 ps simulation, the abundance of H_2O molecule gradually decreases, demonstrating that at high temperature the activity of H_2O molecule is high resulting in the reaction between H_2O and other intermediate products in the decomposition of DNP. In the initial decomposition stage of DNP, there are not N_2 and CO_2 molecules generated, which illustrates that N_2 and CO_2 are produced by the reaction between intermediate products rather than the decomposition of DNP directly.

Experimental detected products are H_2,CH_4,NH_3, H_2O, N_2 and CO_2, which have been detected by ReaxFF MD simulations as well. As the abundance of some products is low such as H_2,CH_4, NH_3, Fig.9 displays the main final products (H_2O, CO_2, N_2) simulated by ReaxFF MD simulations. Fig. 9 illustrates that the increasing temperature enhances the abundance of CO_2 and N_2, demonstrating that high temperature is benefit for the production of CO_2 and N_2. H_2O can react with other unstable fragments to form stable products, which decrease the abundance of H_2O. In addition, the number of total chemical reactions and final products kinds are increased with the increasing temperature, which demonstrates that the higher the temperature is, the more

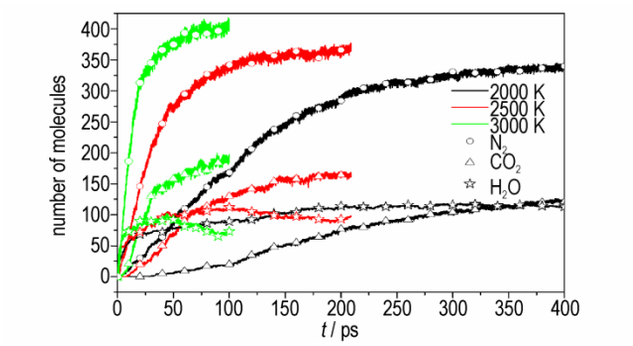

Fig.9 The main final products produced by DNP decomposition at different temperatures

complete the thermal decomposition reaction is.

3.2.4 Reaction kinetic parameter analysis

(1) Initial pyrolysis stage

At different simulation temperature, the k_1 of DNP decomposition are calculated by fitting Eq. 2, and the fitting results are showed in Fig.10. The calculated k_1 of DNP at 2000 K, 2500 K and 3000 K are 0.436 ps^{-1}, 1.075 ps^{-1} and 2.259 ps^{-1}, respectively. With the increase of temperature, the k_1 is increased, illustrating that higher temperature is benefit for enhancing the decomposition rate of the initial decomposition stage of DNP. Then the pre-exponential factor and activation energy of DNP thermal decomposition can be calculated by Eq. 1. The values of A and E_a are 79.38 ps^{-1} and 87.19 $kJ\cdot mol^{-1}$, respectively.

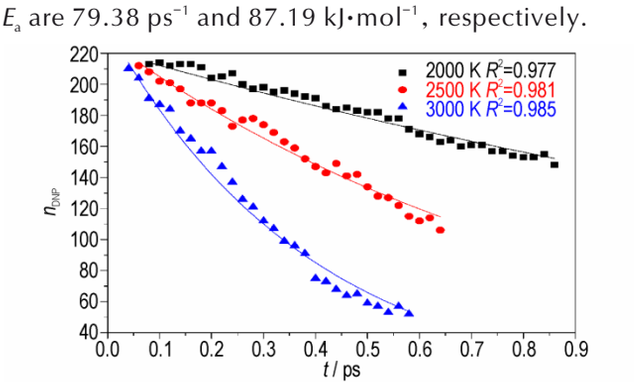

Fig.10 Evolutions of n_{DNP} (point) and their corresponding fitted curves (lines) at different temperatures

(2) Intermediate pyrolysis stage

At different simulation temperature, the k_2 of DNP are calculated by fitting by Eq. 3, and the fitting results are shown in Fig.11. The U_{tmax}, U_∞, t_{max} and calculated k_2 are summarized in Table 4. The calculated k_2 increase with the increasing temperature, illustrating that high temperature can accelerate the intermediate decomposition stage of DNP. Then the pre-exponential factor and activation energy of DNP decomposition can be obtained by Eq. 1. The values of A and E_a are 4.53 ps^{-1} and 108.24 $kJ\cdot mol^{-1}$, respectively.

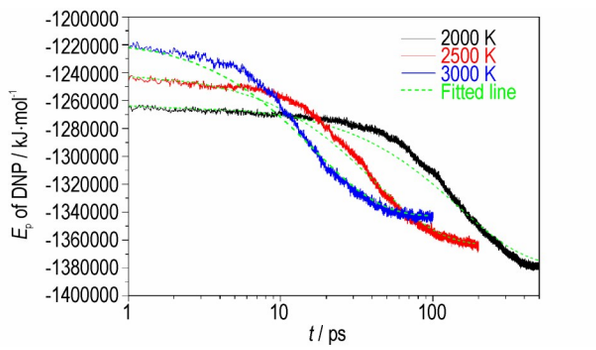

Fig.11 Evolutions of E_p (solid lines) and their corresponding fitted curves (dashed lines) at different temperatures

Table 4 Parameters describing the exponential behaviour of the change of E_p with Time.

T/K	U_{tmax} /kcal·mol^{-1}	U_∞ /kcal·mol^{-1}	t_{max} /ps	k_2 /ps^{-1}
2000	−302612	−329924	0.88	0.0068
2500	−297266	−326515	0.68	0.0241
3000	−291816	−321542	0.60	0.0599

(3) Final product evolution stage

Based on the experimental and simulated results, it can be concluded that the main final products of DNP decomposition at different temperature are N_2, H_2O and CO_2. At different simulation temperature, the k_3 of DNP is calculated by fitting by Eq. 4, and the fitting results are shown in Fig. 12, and asymptotic amounts extracted per product and

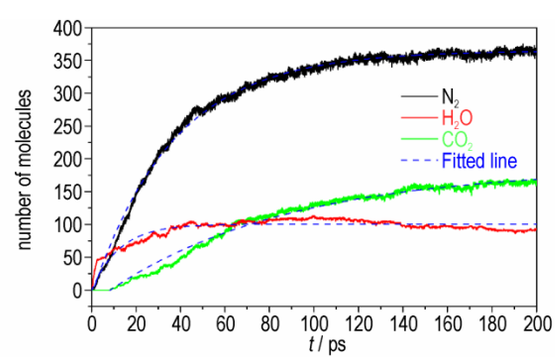

Fig.12 Evolutions of the numbers of N_2, H_2O and CO_2 molecules (solid lines) and their corresponding fitted curves (dash lines) at 2500 K

rate constants are listed in Table 5. Table 5 illustrates that at higher temperature the asymptotic amounts of N_2 and CO_2 are higher, demonstrating that high temperature is benefit for the formation of N_2 and CO_2. However, the asymptotic amount of H_2O decreases with the increasing temperature because of the reaction between H_2O and other intermediate products at high temperature. The calculated k_3 increase with the increasing temperature, illustrating that higher temperature is benefit for the formation of final products during the decomposition of DNP. In addition, at the same temperature the order of k_3 of N_2, H_2O and CO_2 is $H_2O > N_2 > CO_2$, illustrating the formation rates of H_2O is the highest.

Table 5 Final products properties of DNP at 2500 K

Fragment	2000 K		2500 K		3000 K		E_a	A
	C_∞	k_3	C_∞	k_3	C_∞	k_3	/kJ·mol^{-1}	/ps^{-1}
N_2	359	0.0074	364	0.0273	367	0.0697	111.5626	6.0220
H_2O	112	0.0245	100	0.0795	83	0.3176	125.3890	42.1110
CO_2	174	0.0046	186	0.0123	194	0.0302	92.8748	1.1828

3.3 Thermal decomposition mechanisms of DNP

More than 40000 chemical reactions are detected by ReaxFF MD simulations during the decomposition of DNP at all three temperatures, and with the increase of temperature the number of chemical reactions increases. Most of these reactions are the reaction between intermediate products rather than the reaction of DNP, illustrating that the intermediate decomposition stage is main stage during the decomposition of DNP. Actually, the reaction of initial decomposition stage can provide some important information for analysis the decomposition mechanism of DNP. In this study, ReaxFF simulated main chemical reactions and their reaction frequencies in initial 30 ps MD simulation during DNP decomposition are analyzed to obtain the decomposition path of DNP at different temperatures. The simulated main chemical reactions and their frequencies are summarized in Table 6.

Table 6 illustrates that the total number of DNP (216) is lower than the total frequencies of the reaction $C_3H_2O_4N_4 \rightarrow C_3HO_3N_4 + OH$ at 2000 K and 2500 K, because of the formation of $C_3H_2O_4N_4$ by the reaction between unstable intermediate products, and many other the same phenomena exist during the DNP decomposition. At 2000 K and 2500 K the main thermal decomposition path of $C_3HO_3N_4$ is $C_3HO_3N_4 + NO \rightarrow C_3HO_4N_5$. When temperature raise to 3000 K, the main decomposition path of

Table 6 Primary reactions and their frequencies

No.	Primary reactions	Frequencies		
		2000 K	2500 K	3000 K
1	$C_3H_2O_4N_4 \rightarrow C_3HO_3N_4 + OH$	265	247	183
2	$C_3HO_3N_4 \rightarrow C_3HO_2N_3 + NO$	120	82	39
3	$C_3HO_3N_4 \rightarrow C_3HO_3N_2 + N_2$	256	96	33
4	$C_3HO_3N_4 + NO \rightarrow C_3HO_4N_5$	179	73	58
5	$C_3HO_2N_3 \rightarrow C_3HO_2N + N_2$	503	314	150
6	$C_3HO_4N_5 \rightarrow C_3HO_4N_3 + N_2$	100	27	13
7	$C_3HO_4N_3 \rightarrow C_3HO_3N_2 + NO$	76	27	24
8	$C_3HO_3N_2 \rightarrow C_3HO_2N + NO$	68	38	12

$C_3HO_3N_4$ changes to $C_3HO_3N_4 + NO \rightarrow C_3HO_4N_5$. The total reaction frequencies of the above mentioned three paths of $C_3HO_3N_4$ decomposition are decline, demonstrating that some other complex decomposition path of $C_3HO_3N_4$ exist with the increase of temperature. The higher the frequency of the reaction is, the greater the probability of DNP decomposition along this path. At 2000 K and 2500 K the total frequencies of $C_3H_2O_4N_4 \rightarrow C_3HO_3N_4 + OH$ are higher than the total number of DNP (216), illustrating that all DNP are almost decayed along this path. In addition, the increasing temperature decreases the frequencies of all selected reactions (the total number of chemical reactions increase), demonstrating that DNP exists some other complex decomposition path at higher temperature.

Take thermal decomposition of DNP at 2000 K as an example, at the beginning of the simulation,

the main thermal decomposition process of DNP is $C_3H_2O_4N_4 \rightarrow C_3HO_3N_4+OH$. After the formation of $C_3HO_3N_4$, the decomposition processes become complex, and the main process can be summarized into three paths. The first path is the self-decomposition of $C_3HO_3N_4$ to produce NO, i.e. $C_3HO_3N_4 \rightarrow C_3HO_2N_3+NO$. The second is the self-decomposition of $C_3HO_3N_4$ to produce N_2, i.e. $C_3HO_3N_4 \rightarrow C_3HO_3N_2+N_2$. The third path is the reaction between $C_3HO_3N_4$ and NO, i.e. $C_3HO_3N_4+NO \rightarrow C_3HO_4N_5$. At high temperature, $C_3HO_4N_5$ will decompose to $C_3HO_4N_3$ and N_2, i.e. $C_3HO_4N_5 \rightarrow C_3HO_4N_3+N_2$. Then $C_3HO_2N_3$ and $C_3HO_3N_2$ will decompose to $C_3HO_2N+N_2$ and C_3HO_2N+NO, respectively. Finally, C_3HO_2N will decompose to smaller intermediate and final products. Based on the simulation results, the decomposition mechanisms of DNP can be summarized by Scheme 1.

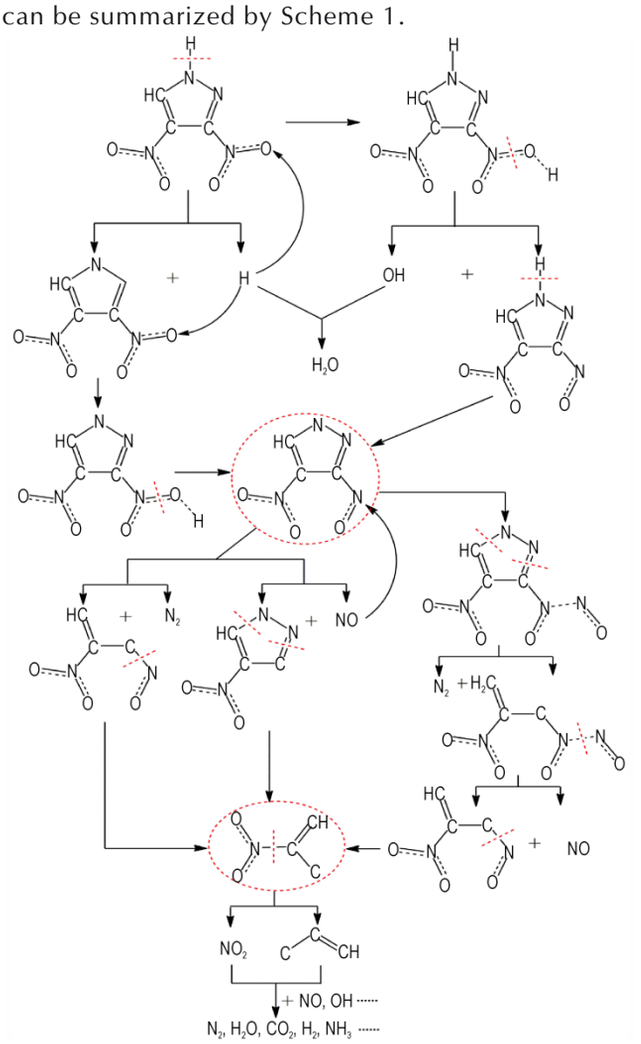

Scheme 1 Thermal decomposition mechanisms of DNP

4 Conclusions

(1) ARC was used to study DNP decomposition properties and to gather the gaseous products, and the gaseous products were identified by MS technique.

(2) ReaxFF MD simulations are performed to investigate the thermal decomposition of DNP at 2000, 2500 and 3000 K.

(3) ARC-MS experiment and ReaxFF MD simulation results show that the final products are H_2O, N_2, CO_2, NH_3 and H_2, and the chronological orders of the appearance final products are $H_2O>N_2>CO_2>NH_3>H_2$.

(4) ReaxFF MD simulation results show that the main intermediate products are $C_3HO_4N_4$, $C_3HO_3N_4$, $C_3HO_2N_3$, C_3HO_2N and NO_2, and the chronological orders of the appearance of intermediate products are $C_3HO_4N_4>C_3HO_3N_4>C_3HO_2N_3>C_3HO_2N>NO_2$.

(5) Based on the main intermediate products, final products and key chemical reactions, the decomposition mechanisms of DNP are obtained.

References:

[1] RAVI P, BADGUJAR D M, GORE G M, et al. Review on melt cast explosives[J]. *Propellants Explosives Pyrotechnics*, 2011, 36(5): 393−403.

[2] BÖLTER M F, HARTER A, KLAPÖTKE T M,et al. Isomers of dinitropyrazoles: Synthesis, comparison and tuning of their physicochemical properties [J]. *Chem Plus Chem*, 2018, 83 (8) : 804−811.

[3] BÖLTER M F, KLAPÖTKE T M, KUSTERMANN T, et al. Improving the energetic properties of dinitropyrazoles by utilization of current concepts [J]. *European Journal of Inorganic Chemistry*, 2018, (37): 4125−4132.

[4] LIU Yang, LI Yong-xiang, LAN Guan-chao, et al. Determination and correlation of solubility of 3,4-dinitro-1H-pyrazole in different pure solvents from 298.15 K to 338.15 K[J]. *Journal of Chemical and Engineering Data*, 2016, 61(7): 2516−2524.

[5] TANG Wei-qiang, REN Hui, JIAO Qing-jie, et al. Property characterization of 3,4-dinitropyrazole and its application[J]. *Chinese Journal of Energetic Materials*, 2017, 25(1): 44−48.

[6] TIAN Xin, LI Jin-shan. Thermal decomposition and non-isothermal kinetics of 3, 4-dinitropyrazole [J]. *Chemical Research and Application*, 2013, 25(2): 206−209.

[7] XIN Li-yong, LIU Chao, LIU Yang, et al. Thermal decomposition mechanism of some hydrocarbons by ReaxFF-based molecular dynamics and density functional theory study[J]. *Fuel*, 2020, 275: 117885.

[8] LIU Qiang, LIU Shi-xiang, LV Ya-dong, et al. Atomic-scale in-

sight into the pyrolysis of polycarbonate by ReaxFF-based reactive molecular dynamics simulation [J]. *Fuel*, 2021, 287: 119484.
[9] YANG Zhi, SUN Yun-jing, MA Fei, et al. Pyrolysis mechanisms of graphene oxide revealed by ReaxFF molecular dynamics simulation[J].*Applied Surface Science*,2020,509: 145247.
[10] PU Yu, LIU Chao, LI Qi-bin, et al. Pyrolysis mechanism of HFO-1234yf with R32 by ReaxFF MD and DFT method[J]. *International Journal of Refrigeration*, 2020, 109: 82-91.
[11] GAO Ming-jie,LI Xiao-xia,GUO Li,et al. Pyrolysis simulations of Fugu coal by large-scale ReaxFF molecular dynamics[J]. *Fuel Processing Technology*, 2018, 178: 197-205.
[12] LI Jing, JIN Shao-hua, LAN Guan-chao, et al. Reactive molecular dynamics simulations on the thermal decompositions and oxidations of TKX-50 and twinned TKX-50 [J]. *Cryst Eng Comm*, 2020, 22(15): 2593-2600.
[13] WEN Yu-shi, XUE Xiang-gui, LONG Xin-ping, et al. Twin induced sensitivity enhancement of HMX versus shock: a molecular reactive force field simulation [J]. *Journal of Physical Chemistry C*, 2013, 117(46): 24368-24374.
[14] ZHANG Lu-zheng, Zybin S V, Duin A C T, et al. Carbon cluster formation during thermal decomposition of octahydro-1,3,5,7-tetranitro-1,3,5,7-tetrazocine and 1,3,5-triamino-2,4,6-trinitrobenzene high explosives from ReaxFF reactive molecular dynamics simulations[J]. *Journal of Physical Chemistry A*, 2009, 113(40): 10619-10640.
[15] WEN Yu-shi, XUE Xiang-gui, LONG Xin-ping, et al. Cluster evolution at early stages of 1,3,5-triamino-2,4,6-trinitrobenzene under various heating conditions: A molecular reactive force field study[J]. *Journal of Physical Chemistry A*, 2016, 120(22): 3929-3937.
[16] REN Chun-xing, LI Xiao-xia, GUO Li. Reaction mechanisms in the thermal decomposition of CL-20 revealed by ReaxFF molecular dynamics simulations[J]. *Acta Physico-Chimica Sinica*, 2018, 34(10): 1151-1162.
[17] GUO De-zhou, AN Qi, Zybin S V, ET AL. The co-crystal of TNT/CL-20 leads to decreased sensitivity toward thermal decomposition from first principles based reactive molecular dynamics[J]. *Journal of Materials Chemistry A*, 2015, 3(10): 5409-5419.
[18] WANG Fu-ping, CHEN Lang, GENG De-shen, et al. Thermal decomposition mechanism of CL-20 at different temperatures by ReaxFF reactive molecular dynamics simulations[J]. *Journal of Physical Chemistry A*, 2018, 122(16): 3971-3979.
[19] PLIMPTON S J. Fast parallel algorithms for short-range molecular dynamics[J]. *Journal of Computational Physics*, 1995, 117(1): 1-19.
[20] SONG Liang, CHEN Li-zhen, Wang Jian-long, et al. Prediction of crystal morphology of 3,4-Dinitro-1H-pyrazole (DNP) in different solvents [J]. *Journal of Molecular Graphics and Modelling*, 2017, 75: 62-68.
[21] CHENOWETH K, DUIN A C T, GODDARD W A. ReaxFF reactive force field for molecular dynamics simulations of hydrocarbon oxidation[J]. *Journal of Physical Chemistry A*, 2008, 112(5): 1040-1053.
[22] STRACHAN A, DUIN A C T, CHAKRABORTY D, et al. Shock waves in high-energy materials: The initial chemical events in nitramine RDX[J]. *Physical Review Letters*, 2003, 91(9): 098301.
[23] CHEN Lang, WANG He-qi, WANG Fu-ping, et al. Thermal decomposition mechanism of 2,2′,4,4′,6,6′-hexanitrostilbene by ReaxFF reactive molecular dynamics simulations[J]. *Journal of Physical Chemistry C*,2018,122(34):19309-19318.
[24] ZHANG Ting-ting, SHI Yi-ding, HUANG Feng-lei. Thermal decomposition mechanism of β-HMX under high pressures via ReaxFF reactive molecular dynamics simulations [J]. *Acta Physico-Chimica Sinica*, 2012, 28(11): 2605-2615.
[25] LAN Guan-chao, LI Jing, ZHANG Guang-yuan, RUAN Jian, LU Zhi-yan, JIN Shao-hua, CAO Duan-lin, WANG Jian-long. Thermal decomposition mechanism study of 3-nitro-1,2,4-triazol-5-one (NTO): Combined TG-FTIR-MS techniques and ReaxFF reactive molecular dynamics simulations [J]. *Fuel*, 2021, 295: 120655.
[26] ZHANG Chun-yuan, JIN Shao-hua, JI Jia-wei, et al. Thermal hazard assessment of TNT and DNAN under adiabatic condition by using accelerating rate calorimeter (ARC)[J]. *Journal of Thermal Analysis and Calorimetry*, 2018, 131: 89-93.
[27] ROM N, ZYBIN S V, DUIN A C T, et al. Density-dependent liquid nitromethane decomposition: molecular dynamics simulations based on ReaxFF[J]. *Journal of Physical Chemistry A*, 2011, 115(36): 10181-10202.

DNP热分解机理的ReaxFF模拟

兰贯超[1,2],张琳升[1],刘学英[2],晁　慧[2],李志华[2],曹端林[1],王建龙[1]
(1.中北大学化学工程与技术学院, 山西 太原 030051; 2.甘肃银光化学工业集团有限公司, 甘肃 白银 730900)

摘　要: 为了研究3,4-二硝基吡唑(DNP)的热分解特性及机理,基于ReaxFF力场采用反应分子动力学方法对DNP热分解过程中的主要中间产物、最终产物和化学反应进行了模拟。采用绝热加速量热仪(ARC)对DNP进行热分解测试,收集分解产生的最终气体产物,采用质谱(MS)技术对收集到的气体产物进行鉴定。模拟结果表明,$C_3HO_4N_4$、$C_3HO_3N_4$、$C_3HO_2N_3$、C_3HNO_2、NO_2是DNP热分解过程中的主要中间产物,H_2O、CO_2、N_2是主要的最终产物。实验检测到的主要气体产物为H_2O、CO_2、N_2,还检测到部分H_2、O_2和NH_3。根据模拟结果可知$C_3HO_3N_4$为最早生成的中间产物,H_2O为最早生成的最终产物。$C_3HO_3N_4$和N_2分别为中间产物和最终产物,其含量最大。通过分子动力学模拟得到了DNP热分解过程中的主要化学反应。根据得到产物的生成时间、丰度和主要化学反应,推测出了DNP的热分解机理。

关键词: 3,4-二硝基吡唑(DNP);反应分子动力学模拟;ARC-MS技术;热分解机理
中图分类号: TJ55　　**文献标志码:** A　　**DOI:**10.11943/CJEM2021190
(责编:高 毅)